Available online at www.sciencedirect.com
ScienceDirect
Journal of Differential Equations 441 (2025) 113474
Journal of Differential Equations
www.elsevier.com/locate/jde

Threshold convergence to steady states for nonlocal reaction-diffusion equations with time delay in bounded domain

Ming Mei [a,b,c], Lin Yang [d,*], Haifeng Hu [e], Dinghua Xu [f,g,**]

[a] *School of Mathematics and Statistics, Jiangxi Normal University, Nanchang, Jiangxi, 330027, China*
[b] *Department of Mathematics, Champlain College Saint-Lambert, Saint-Lambert, Quebec, J4P 3P2, Canada*
[c] *Department of Mathematics and Statistics, McGill University, Montreal, Quebec, H3A 2K6, Canada*
[d] *Department of Mathematics, Shanghai Maritime University, Shanghai 201306, China*
[e] *School of Mathematics and Statistics, Changchun University, Changchun, Jilin, 130022, China*
[f] *School of Mathematics, Shanghai University of Finance and Economics, Shanghai, 200433, China*
[g] *School of Science, Zhejiang Sci-Tech University, Hangzhou, Zhejiang, 310018, China*

Received 22 March 2025; accepted 24 May 2025
Available online 3 June 2025

Abstract

In this paper, we aim at studying the asymptotic behavior for the time-delayed nonlocal reaction-diffusion equation for population dynamics with Dirichlet boundary condition in $\Omega \subset \mathbb{R}^N$. We recognize that there are threshold convergence results of the solutions which depend on the ecological parameters: the spatial diffusion coefficient $D > 0$, the death rate coefficient $\delta > 0$, the birth rate coefficient $p > 0$, and two principal eigenvalues $0 < \lambda_i < 1$ ($i = 1, 2$) of the linear nonlocal dispersion operators induced by the two different kernels with Dirichlet boundaries, respectively. Precisely, when $0 < \frac{(1-\lambda_2)p}{D\lambda_1+\delta} < 1$, we prove that the solution globally converges to the trivial steady state 0 at the exponential rate. When $1 < \frac{(1-\lambda_2)p}{D\lambda_1+\delta} \le e$, we further prove that the solution globally converges to the non-trivial steady state $\phi(x)$ at the exponential rate, and yet this convergence locally holds if $e < \frac{(1-\lambda_2)p}{D\lambda_1+\delta} < e^2$. The convergence rates are also time-exponential. The proof is based on the Fourier transform and the energy method involving the eigenvalue problems for nonlo-

* Co-corresponding author at: Department of Mathematics, Shanghai Maritime University, Shanghai, 201306, China.
** Co-corresponding author at: School of Mathematics, Shanghai University of Finance and Economics, Shanghai, 200433, China.

E-mail addresses: ming.mei@mcgill.ca (M. Mei), yanglin@shmtu.edu.cn (L. Yang), huhf@ccu.edu.cn (H. Hu), dhxu6708@mail.shufe.edu.cn (D. Xu).

https://doi.org/10.1016/j.jde.2025.113474

cal dispersion equations. Some new techniques and skills for treating the nonlocality and non-monotonicity with restriction in bounded domain are also proposed. Finally, a number of numerical simulations are carried out, which confirm our theoretical results. For $\frac{(1-\lambda_2)p}{D\lambda_1+\delta} > e^2$, the solutions are numerically tested to be oscillating.

MSC: 35K57; 35K61; 35Q92

Keywords: Reaction-diffusion equations; Time delay; Nonlocal effects; Asymptotic behavior; Threshold convergence

1. Introduction

Modeling equations. Of concern is the asymptotic behavior for the Dirichlet problem of the nonlocal reaction-diffusion equation with a time delay arising from population dynamics in ecology [2,21,22,25,27,33]:

$$\begin{cases} \frac{\partial u(t,x)}{\partial t} - D(J_1 * u - u)(t,x) + \delta u(t,x) = (J_2 * b(u))(t-r,x), \quad t>0,\ x\in\Omega, \\ u(t,x)\equiv 0, \quad t>0,\ x\in\mathbb{R}^N\setminus\Omega, \\ u(s,x)=u_0(s,x), \quad s\in[-r,0],\ x\in\Omega, \end{cases} \tag{1.1}$$

where $u(t,x)$ stands for the mature population of single species (after the maturation age $r>0$); the spatial range $\Omega\subset\mathbb{R}^N$ is a bounded and convex domain with a smooth boundary $\partial\Omega$; the constants $D>0$ and $\delta>0$ represent the diffusion rate and death rate for the mature population of the species; $(J_1 * u - u)(t,x)$ is the linear nonlocal diffusion operator,

$$(J_1 * u)(t,x) = \int_{\mathbb{R}^N} J_1(x-y)u(t,y)dy, \tag{1.2}$$

and $J_1(x-y)$ is thought of as the probability distribution of jumping from y-site to x-site; $(J_2 * b(u))(t-r,x)$ is the nonlocal term of birth rate with the time delay r, which is defined as

$$(J_2 * b(u))(t-r,x) = \int_{\mathbb{R}^N} J_2(x-y)b(u(t-r,y))dy, \tag{1.3}$$

the birth function $b(\cdot)$ is of the Nicholson's blowflies form

$$b(u) = pue^{-au}, \quad p>0,\ a>0. \tag{1.4}$$

From the ecological point of view, the nonlocal birth term $(J_2 * b(u))(t-r,x)$ allows for some mobility among the immature population of the species. The typical choice about the kernel $J_2(x)$ is the heat kernel (see [33]); however, we are interested in the more general case. In fact, the kernel $J_1(x)$ in the nonlocal diffusion term and the one $J_2(x)$ in the nonlocal birth term satisfy the following hypothesis

$$J_i \in C(\mathbb{R}^N, \mathbb{R}) \text{ are nonnegative,with } J(0) > 0, \text{ and } \int_{\mathbb{R}^N} J(x)dx = 1, \quad i = 1, 2. \tag{1.5}$$

Remarkably, different from the previous studies [3,4], [10–16], [21–27], [31–34], [38,39], the kernels $J_i(x)$ $(i = 1, 2)$ may not be restricted to be radial and symmetric.

The boundary condition in $(1.1)_2$ is similar to the classical Dirichlet boundary condition and indicates that the exterior of the area Ω inhabited by the species is hostile. To put it another way, this is the case when individuals of the species land in $\mathbb{R}^N \setminus \Omega$, they die immediately, thereby resulting in $u(t, x) \equiv 0, x \in \mathbb{R}^N \setminus \Omega$; in contrast to the classical Dirichlet boundary condition, here we do not prescribe the boundary value on $\partial\Omega$, and we accept that the solution $u(t, x)$ might have a discontinuity on $\partial\Omega$.

Background of study. The nonlocal diffusion problems have been used to model very different applied situations, for example in nonlocal anisotropic models for phase transition [1,5], mathematical finances using optimal control theory [7,26], particle systems [8], biology [9,30], coagulation models [18], image processing [20,28], etc. For the non-delayed nonlocal diffusion equations, these equations have been extensively studied in [2,4,6,17,24,25] for the existence, uniqueness and asymptotic behavior of the solutions in bounded/unbounded domains, and in [19,37] for the blowup phenomenon, as well as in [3,12–16] for the structure of traveling waves and their stability, respectively. For the time-delayed nonlocal dispersion equations, the existence of monotone/non-monotone traveling waves were established in [31,38], respectively. The asymptotic stability of these wavefronts were shown in [31] for the case with large wave speed by the weighted energy method, and in [21] for the case of critical waves by the technique combining the weighted energy method and the Fourier transform. When the targeted equation lacks the monotonicity, the traveling waves were proved to be oscillating once the time-delay is large (cf. [23,38]). The global stability of these oscillating critical/non-critical waves with optimal convergence rates were further technically proved by the anti-weighted energy method and the Green function method in [21,32,36,39], independently. The threshold results for the solutions with the local birth rate term in unbounded domain was studied recently in [22]. When the subjected domain is bounded, the asymptotic behavior of the solutions to the time-delayed nonlocal dispersion equations was first studied in [34] for the local case only, and recently investigated in [27] where the term for the birth rate is also isolated locally in one point x only, and the birth rate was restricted to be monotonic.

Main purpose and difficulties. In this paper, we study the dispersion equation (1.1) with nonlocality for both the spatial diffusion and the birth rate, where the birth rate function $b(u)$ can be allowed to be non-monotonic. We are going to prove the threshold convergence results of the solutions according to different values of parameters for the birth rate coefficient p, the death rate coefficient δ, the nonlocal space dispersion coefficient D, and two principal eigenvalues $0 < \lambda_i < 1$ related to the kernels $J_i(x)$ for $i = 1, 2$. Namely, when $0 < \frac{(1-\lambda_2)p}{D\lambda_1+\delta} < 1$, the solution globally converges to the trivial steady state 0 at the exponential rate. This means the single species will become extinct after long time. When $\frac{(1-\lambda_2)p}{D\lambda_1+\delta} > 1$, we prove that there exists a non-trivial steady-state $\phi(x)$ of (1.1). Then we further prove that, when $1 < \frac{(1-\lambda_2)p}{D\lambda_1+\delta} \le e$, the solution globally converges to the non-trivial steady state $\phi(x)$ at the exponential rate, and yet this convergence locally holds if $e < \frac{(1-\lambda_2)p}{D\lambda_1+\delta} < e^2$. This means that the population of the single species will become steady-state after long time. The adopted proof approach is the Fourier transform with the energy estimates. The main difficulties for the study come from two sides. One is from the non-monotonicity of the birth rate function, and the other is from the nonlocalities of the spatial dispersion and the birth rate term. To overcome these difficulties, we treat the problem based on the monotonic/non-monotonic cases of the birth rate, and adopt the energy method with the help of the monotonic technique for the monotonic case to get the global convergence result, and adopt the Fourier analysis and the compactness analysis for the non-monotonic case to show the local convergence result. Furthermore, we use the numerical integration and numerical differentiation techniques to carry out some numerical computations in different cases. These numerical simulations confirm our theoretical results. This is first frame work to show the threshold convergence of the solution to the nonlocal dispersion equations in the bounded domain, which involves the principal eigenvalues. Regarding the case of $\frac{(1-\lambda_2)p}{D\lambda_1+\delta} \geq e^2$, as numerically showed in [11,29,36], when the time-delay r is large, we expect that the solutions occur Hopf bifurcation with infinitely many oscillations. But this case is more challenging, and still keeps open.

It is interesting to compare our threshold results for the initial-boundary value problem in the bounded domain with the results obtained in [22] for the Cauchy problem in full space $\mathbb{R}^N$. There are three different technical issues from [22]. The first issue is about the kernels $J_i(x)$. The kernels are usually assumed to be symmetric and radial in the previous studies including [22], however, such restrictions are removed in this paper. The second issue is about the asymptotic profiles. The threshold asymptotic states in [22] are trivial: $u = 0$ for $0 < \frac{p}{\delta} < 1$ and $u = \frac{1}{a} \ln \frac{p}{\delta} > 0$ for $1 < \frac{p}{\delta} < e^2$. Of course, these states are differentiable in $\mathbb{R}^N$. However, the expected asymptotic profiles considered in this paper for the bounded domain are $u = 0$ for $0 < \frac{(1-\lambda_2)p}{D\lambda_1+\delta} < 1$ and

$$u = \phi(x) = \begin{cases} \frac{1}{a} \ln \frac{(1-\lambda_2)p}{D\lambda_1+\delta}, & x \in \Omega, \\ 0, & x \in \mathbb{R}^N/\Omega, \end{cases}$$

for $1 < \frac{(1-\lambda_2)p}{D\lambda_1+\delta} < e^2$. Obviously, the steady state $\phi(x)$ is non-trivial, and it is discontinuous on the boundary $\partial\Omega$. The third issue is that, the Fourier transform adopted in [22] in the full space $\mathbb{R}^N$ cannot be directly applied to the bounded domain $\Omega \subset \mathbb{R}^N$. To do so, here we heuristically extend the solutions to be zero in the outer region of $\mathbb{R}^N/\Omega$. Such bounded solutions with discontinuity on the boundary are in $L^1(\mathbb{R}^N)$ and their Fourier transforms can be well-defined, however, their inverse Fourier transforms do not exist. This makes the treatment used in the case of full space $\mathbb{R}^N$ in [22] cannot be applied. In order to overcome it, we technically establish the desired energy estimates by the Plancherel equality. We note that, to carry out the energy estimates related to eigenvalues in the bounded domain Ω is more complicated than the case of the full space $\mathbb{R}^N$. So, this paper can be regarded as a significant development to the previous study [22].

The rest of the paper is organized as follows. In Section 2, we first give some preliminaries which will be frequently used in the proofs of the main theorems. In Section 3, we show the existence and uniqueness of the non-trivial steady state if $\frac{(1-\lambda_2)p}{D\lambda_1+\delta} > 1$. In Section 4, we prove that the trivial steady state 0 is globally attractive if $0 < \frac{(1-\lambda_2)p}{D\lambda_1+\delta} < 1$. In Section 5, we further consider the asymptotic stability of the non-trivial steady state if $1 < \frac{(1-\lambda_2)p}{D\lambda_1+\delta} < e^2$. Section 6 provides the reader with some numerical simulations in order to better understand our theoretical results. In the end, we will have some discussions on the obtained theoretical and numerical results which can perfectly interpret the ecological phenomena to the dynamical model of populations in Section 7.

2. Preliminaries

In this section, we begin with some preliminaries concerning the Fourier transform. We assume that the reader is familiar with them and hence we refer to [35] for details. In what follows, $\hat{f}$ denotes the Fourier transform of $f \in L^1(\mathbb{R}^N)$, which is given by the following definition

$$F[f](\xi) = \hat{f}(\xi) = \int_{\mathbb{R}^N} e^{-ix\cdot\xi} f(x)dx, \quad i = \sqrt{-1}. \tag{2.1}$$

Moreover, if $\hat{f} \in L^1(\mathbb{R}^N)$, then the inverse Fourier transform is given by

$$F^{-1}[\hat{f}](x) = \frac{1}{(2\pi)^N} \int_{\mathbb{R}^N} e^{ix\cdot\xi} \hat{f}(\xi)d\xi. \tag{2.2}$$

In the following proposition we list some of the main properties of the Fourier transform and its inverse transform.

Proposition 2.1.

(1) $\widehat{f * g} = \hat{f} \cdot \hat{g}$.
(2) *(Fourier Inversion Theorem) For $f \in L^1(\mathbb{R}^N)$ such that $\hat{f} \in L^1(\mathbb{R}^N)$, the inversion formula*

$$f(x) = F^{-1}[\hat{f}](x)$$

holds for almost every $x \in \mathbb{R}^N$.

Also, we state a useful result (see [10]) related to the following eigenvalue problem with the homogeneous Dirichlet boundary condition:

$$\begin{cases} -(J * \phi - \phi)(x) = \lambda\phi(x), & x \in \Omega, \\ \phi(x) = 0, & x \in \mathbb{R}^N \setminus \Omega. \end{cases} \tag{2.3}$$

Proposition 2.2. *Let $\Omega \subset \mathbb{R}^N$ be a bounded and convex domain with a smooth boundary, and assume that the kernel $J(x)$ satisfies the hypothesis (1.5). Then the principle eigenvalue of (2.3) can be represented by*

$$\lambda_p(\Omega) = \inf_{u \in L^2(\Omega)} \frac{\frac{1}{2}\int_{\mathbb{R}^N}\int_{\mathbb{R}^N} J(x-y)(\bar{u}(x) - \bar{u}(y))^2 dxdy}{\int_\Omega u^2 dx}, \tag{2.4}$$

where $\bar{u}(x)$ is the zero-padding of $u(x)$ outside Ω. Moreover, denote by $\phi_p(x)$ a corresponding non-negative function. Then $\phi_p(x)$ is strictly positive in Ω and λ_p is a positive simple eigenvalue with $0 < \lambda_p < 1$.

Remark 2.1. Observe that the first eigenfunction $\phi_p(x)$ is strictly positive in Ω (with a positive continuous extension to $\overline{\Omega}$) and vanishes outside Ω. Therefore a discontinuity occurs on $\partial\Omega$ and the boundary value is not taken in the usual “classical” sense.

3. Steady-state solutions

Note that the corresponding steady state problem of (1.1) is given by

$$\begin{cases} -D(J_1 * \phi - \phi)(x) + \delta\phi(x) = [J_2 * b(\phi)](x), & x \in \Omega, \\ \phi(x) = 0, & x \in \mathbb{R}^N \setminus \Omega. \end{cases} \tag{3.1}$$

Obviously, the constant equilibrium $\phi(x) \equiv 0$ is a trivial solution of (3.1). Here we are mainly interested in the non-trivial steady state.

First of all, let us look at the following two eigenvalue problems associated by the steady state problem (3.1): for $i = 1, 2$,

$$\begin{cases} -(J_i * \phi_i - \phi_i)(x) = \lambda_i \phi_i(x), & x \in \Omega, \\ \phi_i(x) = 0, & x \in \mathbb{R}^N \setminus \Omega. \end{cases} \tag{3.2}$$

Applying the result in Proposition 2.2 to the eigenvalue problem (3.2), we know that for $i = 1, 2$ there is a principal eigenpair $(\lambda_i, \phi_i(x))$ with $0 < \lambda_i < 1$ and $\phi_i(x) > 0$ in Ω.

We are now in a position to state our main result about the non-trivial steady state.

Theorem 3.1 *(Steady states). Except the trivial solution $\phi(x) \equiv 0$ to (3.1), there exists a nontrivial steady-state to (3.1):*

$$\phi(x) = \begin{cases} \frac{1}{a} \ln \frac{(1-\lambda_2)p}{D\lambda_1 + \delta}, & x \in \Omega, \\ 0, & x \in \mathbb{R}^N \setminus \Omega, \end{cases} \tag{3.3}$$

provided with

$$\frac{(1-\lambda_2)p}{D\lambda_1 + \delta} > 1. \tag{3.4}$$

Proof. As similarly showed in [27], the solution $\phi(x)$ of the equation (3.1) is bounded for $x \in \Omega$. So $\phi \in L^1(\mathbb{R}^N)$, because $\phi(x) \equiv 0$ for $x \in \mathbb{R}^N/\Omega$.

Taking the Fourier transform, the steady state problem (3.1) and the corresponding eigenvalue problem (3.2) can be recast as

$$-D(\hat{J}_1 - 1)\hat{\phi} + \delta\hat{\phi} = \hat{J}_2 \widehat{b(\phi)}, \tag{3.5}$$

and

$$-(\hat{J}_i - 1)\hat{\phi}_i = \lambda_i \hat{\phi}_i, \quad \text{for } i = 1, 2, \tag{3.6}$$

where (λ_i, ϕ_i) is the principal eigenpair of (3.2), and we also make no distinction between solutions and their zero-paddings.

Multiplying (3.5) by $\hat{\phi}_1\hat{\phi}_2$, then we have

$$-D(\hat{J}_1 - 1)\hat{\phi}_1\hat{\phi}_2\hat{\phi} + \delta\hat{\phi}_1\hat{\phi}_2\hat{\phi} = \hat{J}_2\hat{\phi}_2\hat{\phi}_1\widehat{b(\phi)},$$

which in turn gives us

$$D\lambda_1\hat{\phi}_1\hat{\phi}_2\hat{\phi} + \delta\hat{\phi}_1\hat{\phi}_2\hat{\phi} = (1-\lambda_2)\hat{\phi}_2\hat{\phi}_1\widehat{b(\phi)} \tag{3.7}$$

by using (3.6).

Since $\hat{\phi}_1 \neq 0$ and $\hat{\phi}_2 \neq 0$, then

$$(D\lambda_1 + \delta)\hat{\phi} = (1-\lambda_2)\widehat{b(\phi)}. \tag{3.8}$$

Since $\hat{\phi} \notin L^1(\mathbb{R}^N)$, the inverse Fourier transform of $\hat{\phi}$ may not exist, and we cannot take the inverse Fourier transform to (3.8). We need to treat it in a different way. Let us square both sides of (3.8), and integrate it over $\mathbb{R}^N$, then we have

$$(D\lambda_1 + \delta)^2 \int_{\mathbb{R}^N} |\hat{\phi}(\xi)|^2 d\xi = (1-\lambda_2)^2 p^2 \int_{\mathbb{R}^N} |\widehat{\phi e^{-a\phi}}|^2 d\xi. \tag{3.9}$$

By the Plancherel Theorem: $\|\hat{f}\|_{L^2} = \|f\|_{L^2}$, from (3.9) we have

$$(D\lambda_1 + \delta)^2 \int_{\mathbb{R}^N} |\phi(x)|^2 dx = (1-\lambda_2)^2 p^2 \int_{\mathbb{R}^N} |\phi(x) e^{-a\phi(x)}|^2 dx. \tag{3.10}$$

Namely, it is

$$\int_{\mathbb{R}^N} |\phi(x)|^2 \Big[(D\lambda_1 + \delta)^2 - (1-\lambda_2)^2 p^2 e^{-2a\phi(x)}\Big] dx = 0. \tag{3.11}$$

Obviously, it can be checked that $\phi(x) \equiv 0$ is a trivial solution to (3.11), and a non-trivial solution to (3.11) is

$$\phi(x) = \begin{cases} \frac{1}{a}\ln\frac{(1-\lambda_2)p}{D\lambda_1+\delta}, & x \in \Omega, \\ 0, & x \in \mathbb{R}^N \setminus \Omega, \end{cases}$$

provided with $\frac{(1-\lambda_2)p}{D\lambda_1+\delta} > 1$. The proof is complete. $\square$

4. Case of $0 < \frac{(1-\lambda_2)p}{D\lambda_1+\delta} < 1$: global convergence to 0

In this section, we start to consider the large time behavior of solutions to the time-dependent problem (1.1). To this end, we first state the existence and uniqueness of global solutions to the problem (1.1). We will omit the proof, because it is exactly in the same way as [27] (P5690, Theorem 3.1).

Lemma 4.1 *(Global existence and uniqueness). Let $u_0 \in C_+([-r, 0] \times \Omega)$. Then the unique solution to the problem* (1.1) *globally exists in the function space:*

$$u \in C_+(\mathbb{R}_+ \times \Omega), \quad u_t \in C(\mathbb{R}_+ \times \Omega). \tag{4.1}$$

Next we can state our main result in the case of $0 < \frac{(1-\lambda_2)p}{D\lambda_1+\delta} < 1$.

Theorem 4.1 *(Global convergence to the trivial steady state). If $u_0 \in C_+([-r,0]\times\Omega)$ and $0 < \frac{(1-\lambda_2)p}{D\lambda_1+\delta} < 1$, then the solution $u(t,x)$ to the problem (1.1) globally converges to 0 as follows:*

$$\|u(t)\|_{L^2(\Omega)} \le C\left(\|u_0(0)\|_{L^2(\Omega)} + \|u_0\|_{L^2([-r,0];L^2(\Omega))}\right)e^{-\mu t}, \tag{4.2}$$

where $C>0$ and $\mu>0$ are constants, and μ satisfies

$$0 < \mu < (D\lambda_1+\delta) - (1-\lambda_2)p.$$

Proof. We prove (4.2) when $0 < \frac{(1-\lambda_2)p}{D\lambda_1+\delta} < 1$. From Lemma 4.1, the solution $u \in C_+(\mathbb{R}_+\times\Omega)$ of the equation (1.1) is bounded. Note that $u(t,x)\equiv 0$ for $x \in \mathbb{R}^N\setminus\Omega$ and $t>0$, then $u \in L^1(\mathbb{R}^N)$. Taking the Fourier transform to the problem (1.1), we have

$$\frac{d\hat{u}}{dt} - D(\hat{J}_1 - 1)\hat{u} + \delta\hat{u} = \hat{J}_2\widehat{b(u)}. \tag{4.3}$$

Multiplying through (4.3) by $\hat{\phi_1}\hat{\phi_2}$, (λ_i,ϕ_i) are the principal eigenpairs of (3.2) for $i=1,2$, we calculate that

$$\begin{aligned}
&\frac{d\hat{u}}{dt}\hat{\phi_1}\hat{\phi_2} - D(\hat{J}_1-1)\hat{u}\hat{\phi_1}\hat{\phi_2} + \delta\hat{u}\hat{\phi_1}\hat{\phi_2} = \hat{J}_2\widehat{b(u)}\hat{\phi_1}\hat{\phi_2}\\
&\frac{d\hat{u}}{dt}\hat{\phi_1}\hat{\phi_2}\underbrace{-D(\hat{J}_1-1)\hat{\phi_1}}\hat{u}\hat{\phi_2} + \delta\hat{u}\hat{\phi_1}\hat{\phi_2} = \underbrace{\hat{J}_2\hat{\phi_2}}\widehat{b(u)}\hat{\phi_1}
\end{aligned}$$

$$\frac{d\hat{u}}{dt}\hat{\phi_1}\hat{\phi_2} + (D\lambda_1+\delta)\hat{u}\hat{\phi_1}\hat{\phi_2} = (1-\lambda_2)\widehat{b(u)}\hat{\phi_1}\hat{\phi_2},$$

where we have used the fact that $-D(\hat{J}_1-1)\hat{\phi_1} = D\lambda_1\hat{\phi_1}$ and $\hat{J}_2\hat{\phi_2} = (1-\lambda_2)\hat{\phi_2}$. Note that $\hat{\phi_1}\neq 0$ and $\hat{\phi_2}\neq 0$, we further get

$$\frac{d\hat{u}}{dt} + (D\lambda_1+\delta)\hat{u} = (1-\lambda_2)\widehat{b(u)}. \tag{4.4}$$

Multiplying (4.4) by $e^{2\mu t}\hat{u}$ with some constant $\mu>0$ to be determined later, and integrating the resultant equation over $[0,t]\times\mathbb{R}^N$, we have

$$\begin{aligned}
&e^{2\mu t}\|\hat{u}(t)\|^2_{L^2(\mathbb{R}^N)} + 2(D\lambda_1+\delta-\mu)\int_0^t e^{2\mu s}\|\hat{u}(s)\|^2_{L^2(\mathbb{R}^N)}ds\\
&= \|\hat{u}_0(0)\|^2_{L^2(\mathbb{R}^N)} + 2(1-\lambda_2)p\int_0^t e^{2\mu s}\int_{\mathbb{R}^N}\hat{u}(s,\xi)\widehat{ue^{-au}}(s-r,\xi)d\xi ds.
\end{aligned} \tag{4.5}$$

Using the Cauchy-Schwarz inequality, the Plancherel equality, the positiveness of $u \geq 0$, and the change of variable $s - r \to s$, we can estimate the last term of (4.5) as

$$
\begin{aligned}
&2(1-\lambda_2)p\Big|\int_0^t e^{2\mu s}\int_{\mathbb{R}^N}\hat{u}(s,\xi)\widehat{ue^{-au}}(s-r,\xi)d\xi ds\Big| \\
&\leq 2(1-\lambda_2)p\int_0^t e^{2\mu s}\int_{\mathbb{R}^N}\left[\frac{1}{2}|\hat{u}(s,\xi)|^2+\frac{1}{2}|\widehat{ue^{-au}}(s-r,\xi)|^2\right]d\xi ds \\
&=(1-\lambda_2)p\int_0^t e^{2\mu s}\Big[\|\hat{u}(s)\|^2_{L^2(\mathbb{R}^N)}+\|\widehat{ue^{-au}}(s-r)\|^2_{L^2(\mathbb{R}^N)}\Big]ds \\
&=(1-\lambda_2)p\int_0^t e^{2\mu s}\Big[\|u(s)\|^2_{L^2(\mathbb{R}^N)}+\|ue^{-au}(s-r)\|^2_{L^2(\mathbb{R}^N)}\Big]ds \\
&=(1-\lambda_2)p\int_0^t e^{2\mu s}\|u(s)\|^2_{L^2(\Omega)}ds+(1-\lambda_2)p\int_0^t e^{2\mu s}\int_\Omega u^2(s-r,x)e^{-2au(s-r,x)}dxds \\
&\leq (1-\lambda_2)p\int_0^t e^{2\mu s}\|u(s)\|^2_{L^2(\Omega)}ds+(1-\lambda_2)p\int_0^t e^{2\mu s}\int_\Omega u^2(s-r,x)dxds \\
&=(1-\lambda_2)p\int_0^t e^{2\mu s}\|u(s)\|^2_{L^2(\Omega)}ds+(1-\lambda_2)p\int_{-r}^{t-r} e^{2\mu(s+r)}\int_\Omega u^2(s,x)dxds \\
&\leq (1-\lambda_2)p(1+e^{2\mu r})\int_0^t e^{2\mu s}\|u(s)\|^2_{L^2(\Omega)}ds+(1-\lambda_2)p\int_{-r}^{0} e^{2\mu(s+r)}\|u_0(s)\|^2_{L^2(\Omega)}ds. \quad (4.6)
\end{aligned}
$$

Substituting (4.6) to (4.5), and applying the Plancherel equality $\|\hat{u}(t)\|^2_{L^2(\mathbb{R}^N)} = \|u(t)\|^2_{L^2(\mathbb{R}^N)} = \|u(t)\|^2_{L^2(\Omega)}$ because of $u \equiv 0$ for $x \in \mathbb{R}^N \setminus \Omega$, then we obtain

$$
\begin{aligned}
&e^{2\mu t}\|u(t)\|^2_{L^2(\Omega)}+A(\mu)\int_0^t e^{2\mu s}\|u(s)\|^2_{L^2(\Omega)}ds \\
&\leq \|u_0(0)\|^2_{L^2(\Omega)}+(1-\lambda_2)p\int_{-r}^0 e^{2\mu(s+r)}\|u_0(s)\|^2_{L^2(\Omega)}ds, \quad (4.7)
\end{aligned}
$$

where

$$
A(\mu) := 2(D\lambda_1+\delta)-\mu-(1-\lambda_2)p(1+e^{2\mu r}).
$$

Since $(D\lambda_1+\delta)>(1-\lambda_2)p$, then a small number of $\mu>0$ can be solved from the equation

$$A(\mu)=2(D\lambda_1+\delta)-\mu-(1-\lambda_2)p(1+e^{2\mu r})=0.$$

Thus, (4.7) implies

$$\|u(t)\|_{L^2(\Omega)}\le C\left(\|u_0(0)\|_{L^2(\Omega)}+\|u_0\|_{L^2([-r,0];L^2(\Omega))}\right)e^{-\mu t}.$$

The proof is complete. □

5. Case of $1<\frac{(1-\lambda_2)p}{D\lambda_1+\delta}<e^2$: convergence to the non-trivial steady state

In this section, we further consider the large time behavior of solutions to the problem (1.1) in the case of $1<\frac{(1-\lambda_2)p}{D\lambda_1+\delta}<e^2$. Up to now, we have showed there exists a unique non-trivial steady state (see (3.3))

$$\phi(x)=\begin{cases}u_+, & x\in\Omega,\\ 0, & x\in\mathbb{R}^N\setminus\Omega,\end{cases} \tag{5.1}$$

where $u_+:=\frac{1}{a}\ln\frac{(1-\lambda_2)p}{D\lambda_1+\delta}>0$.

We are now in a position to state our main result in the case of $1<\frac{(1-\lambda_2)p}{D\lambda_1+\delta}<e^2$. In fact, it consists of two parts: one is for the global convergence; the other is for local convergence.

Theorem 5.1. *Assume that $u_0\in C_+([-r,0]\times\Omega)$ and $0\le u_0\le\frac{1}{a}$.*

- *If $1<\frac{(1-\lambda_2)p}{D\lambda_1+\delta}\le e$, then the solution $u(t,x)$ to the problem (1.1) globally converges to the non-trivial steady state $\phi(x)$ at the exponential decay rate*

$$\|(u-\phi)(t)\|_{L^2(\Omega)}\le Ce^{-\eta t}, \tag{5.2}$$

  where C and η are positive constants.
- *If $e<\frac{(1-\lambda_2)p}{D\lambda_1+\delta}<e^2$, then the solution $u(t,x)$ locally converges to the non-trivial steady state $\phi(x)$ in the exponential form*

$$\|(u-\phi)(t)\|_{L^2(\Omega)}\le Ce^{-\gamma t} \tag{5.3}$$

  provided $\|(u_0-\phi)(0)\|_{L^2(\Omega)}+\|u_0-\phi\|_{L^2([-r,0];L^2(\Omega))}$ is small enough, where C and γ are positive constants.

Proof. We first prove the global convergence result (5.2) in the case of $1<\frac{(1-\lambda_2)p}{D\lambda_1+\delta}\le e$. Noting that $0\le u_0(s,x)\le\frac{1}{a}$, we can easily know that

$$0\le u(t,x)\le\frac{1}{a},\quad \forall t\ge -r,\ x\in\Omega.$$

Now, we set

$$u_0^+(s,x) := \max_{\substack{x\in\Omega\\ s\in[-r,0]}} \{u_0(s,x), u_+\}, \quad u_0^-(s,x) := \min_{\substack{x\in\Omega\\ s\in[-r,0]}} \{u_0(s,x), u_+\}.$$

Then $u_0^+(s,x)$ and $u_0^-(s,x)$ satisfy

$$0 \le u_0^-(s,x) \le u_+ \le u_0^+(s,x) \le \frac{1}{a}, \quad \forall (s,x) \in [-r,0]\times\Omega.$$

Replacing the initial value $u_0(s,x)$ in the problem (1.1) by $u_0^+(s,x)$ and $u_0^-(s,x)$, and denoting the corresponding solutions by $U^+(t,x)$ and $U^-(t,x)$, we have

$$\begin{cases} \frac{\partial U^\pm(t,x)}{\partial t} - D(J_1 * U^\pm - U^\pm)(t,x) + \delta U^\pm(t,x) \\ \qquad\qquad\qquad = J_2 * b\left(U^\pm(t-r,x)\right), \quad t>0, x\in\Omega, \\ U^\pm(t,x) \equiv 0, \quad t>0,\ x\in\mathbb{R}^N\setminus\Omega, \\ U^\pm(s,x) = u_0^\pm(s,x), \quad s\in[-r,0],\ x\in\Omega. \end{cases} \tag{5.4}$$

From the comparison theorem [22,27], it is easy to see that

$$\begin{cases} 0 \le U^-(t,x) \le u_+ \le U^+(t,x) \le \frac{1}{a}, \\ 0 \le U^-(t,x) \le u(t,x) \le U^+(t,x) \le \frac{1}{a}. \end{cases} \tag{5.5}$$

Similarly to (4.4), we can also reduce (5.4) for $U^+(t,x)$ to the following form:

$$\frac{\partial \widehat{U^+}(t,\xi)}{\partial t} + (D\lambda_1+\delta)\widehat{U^+}(t,\xi) = (1-\lambda_2)\widehat{b(U^+)}(t-r,\xi), \quad t>0,\ \xi\in\mathbb{R}^N. \tag{5.6}$$

Besides, it is obvious that

$$(D\lambda_1+\delta)u_+ = (1-\lambda_2)b(u_+), \tag{5.7}$$

and

$$(D\lambda_1+\delta)\phi(x) = (1-\lambda_2)b(\phi(x)), \quad x\in\mathbb{R}^N. \tag{5.8}$$

Taking Fourier transform to (5.8), we have

$$(D\lambda_1+\delta)\hat{\phi}(\xi) = (1-\lambda_2)\widehat{b(\phi)}(\xi), \quad \xi\in\mathbb{R}^N. \tag{5.9}$$

Defining

$$V^+(t,x) := U^+(t,x) - \phi(x) = \begin{cases} U^+(t,x) - u_+, & \text{for } x\in\Omega, \\ 0, & \text{for } x\in\mathbb{R}^N\setminus\Omega \end{cases} \tag{5.10}$$

and subtract (5.9) from (5.6), we have

$$\frac{\partial \widehat{V^+}(t,\xi)}{\partial t} + (D\lambda_1+\delta)\widehat{V^+}(t,\xi) = (1-\lambda_2)\mathcal{F}[b(\phi+V^+)-b(\phi)](t-r,\xi), \quad t>0,\ \xi\in\mathbb{R}^N. \tag{5.11}$$

Here, we denote $\mathcal{F}[b(\phi+V^+)-b(\phi)]$ as Fourier transform of $b(\phi+V^+)-b(\phi)$.

Multiplying (5.11) by $e^{2\eta t}\widehat{V^+}$ with some constant $\eta>0$ to be determined later, integrating it over $[0,t]\times\mathbb{R}^N$, and using Hölder inequality, we have

$$\begin{aligned}
&e^{2\eta t}\|\widehat{V^+}(t)\|^2_{L^2(\mathbb{R}^N)} + 2(D\lambda_1+\delta-\eta)\int_0^t e^{2\eta s}\|\widehat{V^+}(s)\|^2_{L^2(\mathbb{R}^N)}ds \\
&= \|\widehat{V^+}(0)\|^2_{L^2(\mathbb{R}^N)} + 2(1-\lambda_2)\int_0^t e^{2\eta s}\int_{\mathbb{R}^N}\widehat{V^+}(s,\xi)\mathcal{F}[b(\phi+V^+)-b(\phi)](s-r,\xi)d\xi ds \\
&\le \|\widehat{V^+}(0)\|^2_{L^2(\mathbb{R}^N)} \\
&\quad +2(1-\lambda_2)\int_0^t e^{2\eta s}\|\widehat{V^+}(s)\|_{L^2(\mathbb{R}^N)}\|\mathcal{F}[b(\phi+V^+)-b(\phi)](s-r)\|_{L^2(\mathbb{R}^N)}ds.
\end{aligned} \tag{5.12}$$

Applying the Plancherel equality to (5.12), we obtain

$$\begin{aligned}
&e^{2\eta t}\|V^+(t)\|^2_{L^2(\mathbb{R}^N)} + 2(D\lambda_1+\delta-\eta)\int_0^t e^{2\eta s}\|V^+(s)\|^2_{L^2(\mathbb{R}^N)}ds \\
&\le \|V^+(0)\|^2_{L^2(\mathbb{R}^N)} \\
&\quad +2(1-\lambda_2)\int_0^t e^{2\eta s}\|V^+(s)\|_{L^2(\mathbb{R}^N)}\|[b(\phi+V^+)-b(\phi)](s-r)\|_{L^2(\mathbb{R}^N)}ds.
\end{aligned} \tag{5.13}$$

By Taylor's expansion, we have

$$b(\phi+V^+(t-r,x))-b(\phi) = b'(\phi)V^+(t-r,x)+\frac{1}{2}b''(\tilde{u})[V^+(t-r,x)]^2, \tag{5.14}$$

where $\tilde{u}$ is between ϕ and $U^+(t-r,x)$, which in turn implies $0\le\tilde{u}\le\frac{1}{a}$ and $b''(\tilde{u})\le 0$.

When $1<\frac{(1-\lambda_2)p}{D\lambda_1+\delta}\le e$, from (5.5), we have $U^+(t,x)\ge\phi(x)$, and we reduce (5.14) to the following inequality

$$\begin{aligned}
0 &\le b(\phi(x)+V^+(t-r,x))-b(\phi(x)) \\
&\le b'(\phi(x))V^+(t-r,x) \\
&= p(1-a\phi(x))e^{-a\phi(x)}V^+(t-r,x) \\
&= \begin{cases} p(1-au_+)e^{-au_+}V^+(t-r,x), & x\in\Omega, \\ 0, & x\in\mathbb{R}^N\setminus\Omega \end{cases}
\end{aligned}$$

$$= \begin{cases} \frac{D\lambda_1+\delta}{1-\lambda_2}\left(1-\ln\frac{(1-\lambda_2)p}{D\lambda_1+\delta}\right)V^+(t-r,x), & x\in\Omega, \\ 0, & x\in\mathbb{R}^N\setminus\Omega. \end{cases} \tag{5.15}$$

Thus, we have

$$\|(b(\phi+V^+)-b(\phi))(s-r)\|_{L^2(\mathbb{R}^N)} \le \frac{D\lambda_1+\delta}{1-\lambda_2}\left(1-\ln\frac{(1-\lambda_2)p}{D\lambda_1+\delta}\right)\|V^+(s-r)\|_{L^2(\Omega)}. \tag{5.16}$$

From (5.10), we have

$$\|V^+(t)\|_{L^2(\mathbb{R}^N)} = \|V^+(t)\|_{L^2(\Omega)}.$$

Substituting this with (5.16) together to (5.13), we have

$$\begin{aligned} &e^{2\eta t}\|V^+(t)\|^2_{L^2(\Omega)} + 2(D\lambda_1+\delta-\eta)\int_0^t e^{2\eta s}\|V^+(s)\|^2_{L^2(\Omega)}ds \\ &\le \|V^+(0)\|^2_{L^2(\Omega)} \\ &\quad +2(D\lambda_1+\delta)\left(1-\ln\frac{(1-\lambda_2)p}{D\lambda_1+\delta}\right)\int_0^t e^{2\eta s}\|V^+(s)\|_{L^2(\Omega)}\|V^+(s-r)\|_{L^2(\Omega)}ds. \end{aligned} \tag{5.17}$$

Using the Cauchy-Schwarz inequality, and the change of variables $s-r\to s$, we have

$$\begin{aligned} &\int_0^t e^{2\eta s}\|V^+(s)\|_{L^2(\Omega)}\|V^+(s-r)\|_{L^2(\Omega)}ds \\ &\le \frac{1}{2}\int_0^t e^{2\eta s}\|V^+(s)\|^2_{L^2(\Omega)}ds + \frac{1}{2}\int_0^t e^{2\eta s}\|V^+(s-r)\|^2_{L^2(\Omega)}ds \\ &= \frac{1}{2}\int_0^t e^{2\eta s}\|V^+(s)\|^2_{L^2(\Omega)}ds + \frac{1}{2}\int_{-r}^{t-r} e^{2\eta(s+r)}\|V^+(s)\|^2_{L^2(\Omega)}ds \\ &\le \int_0^t e^{2\eta s}\|V^+(s)\|^2_{L^2(\Omega)}ds + \frac{1}{2}\int_{-r}^{0} e^{2\eta(s+r)}\|V^+(0)\|^2_{L^2(\Omega)}ds. \end{aligned} \tag{5.18}$$

Substituting (5.18) into (5.17), we have

$$\begin{aligned} &e^{2\eta t}\|V^+(t)\|^2_{L^2(\Omega)} + B(\eta)\int_0^t e^{2\eta s}\|V^+(s)\|^2_{L^2(\Omega)}ds \\ &\le C(\|V_0^+(0)\|^2_{L^2(\Omega)} + \|V_0^+\|_{L^2([-r,0];L^2(\Omega))}), \end{aligned} \tag{5.19}$$

where

$$\begin{aligned}
B(\eta):=&\,2\bigg[(D\lambda_1+\delta)-(D\lambda_1+\delta)\left(1-\ln\frac{(1-\lambda_2)p}{D\lambda_1+\delta}\right)\\
&\quad-\eta-\frac{1}{2}(D\lambda_1+\delta)\left(1-\ln\frac{(1-\lambda_2)p}{D\lambda_1+\delta}\right)\left(e^{2\eta r}-1\right)\bigg]\\
=&\,2\bigg[(D\lambda_1+\delta)\ln\frac{(1-\lambda_2)p}{D\lambda_1+\delta}\\
&\quad-\eta-\frac{1}{2}(D\lambda_1+\delta)\left(1-\ln\frac{(1-\lambda_2)p}{D\lambda_1+\delta}\right)\left(e^{2\eta r}-1\right)\bigg].
\end{aligned}\tag{5.20}$$

Since $1<\frac{(1-\lambda_2)p}{D\lambda_1+\delta}\le e$, then we have $0<\ln\frac{(1-\lambda_2)p}{D\lambda_1+\delta}\le 1$ and $0\le 1-\ln\frac{(1-\lambda_2)p}{D\lambda_1+\delta}<1$. Thus, we can choose $\eta>0$ which is the unique root of the equation $B(\eta)=0$ such that (5.19) gives

$$\begin{aligned}
\|U^+(t)-\phi\|^2_{L^2(\Omega)}&=\|V^+(t)\|^2_{L^2(\Omega)}\\
&\le C\left(\|V_0^+(0)\|^2_{L^2(\Omega)}+\|V_0^+\|^2_{L^2([-r,0];L^2(\Omega))}\right)e^{-2\eta t}.
\end{aligned}\tag{5.21}$$

Namely,

$$\|U^+(t)-\phi\|_{L^2(\Omega)}\le Ce^{-\eta t}.\tag{5.22}$$

Besides, in the same way, we can establish the following result in much the same way as in (5.22):

$$\|U^-(t)-\phi\|_{L^2(\Omega)}\le Ce^{-\eta t}.\tag{5.23}$$

From (5.5), we have the squeezing relation

$$0\le|u(t,x)-\phi|\le U^+(t,x)-U^-(t,x),\quad t>0,\ x\in\Omega.\tag{5.24}$$

Therefore, it is easy to see that

$$\begin{aligned}
\|(u-\phi)(t)\|_{L^2(\Omega)}&\le\|(U^+-U^-)(t)\|_{L^2(\Omega)}\\
&=\|(U^+-\phi+\phi-U^-)(t)\|_{L^2(\Omega)}\\
&\le\|(U^+-\phi)(t)\|_{L^2(\Omega)}+\|(U^--\phi)(t)\|_{L^2(\Omega)}\\
&\le Ce^{-\eta t}.
\end{aligned}\tag{5.25}$$

Next, we are going to prove the local convergence result (5.3) when $e<\frac{(1-\lambda_2)p}{D\lambda_1+\delta}<e^2$. To this end, we let

$$v(t,x) := u(t,x) - \phi(x) = \begin{cases} u(t,x) - u_+, & x \in \Omega, \\ 0, & x \in \mathbb{R}^N \setminus \Omega. \end{cases}$$

Thus, $v(t,x)$ satisfies

$$\frac{\partial v(t,x)}{\partial t} - D(J_1 * v - v) + \delta v(t,x) = J_2 * [b(\phi + v(t-r,x)) - b(\phi)]. \tag{5.26}$$

Similarly to (5.11), taking Fourier transform to (5.26), we have

$$\frac{\partial \hat{v}(t,\xi)}{\partial t} + (D\lambda_1 + \delta)\hat{v}(t,\xi) = (1-\lambda_2)\mathcal{F}[b(\phi+v) - b(\phi)](t-r,\xi), \tag{5.27}$$

where $\mathcal{F}[b(\phi + v(t-r,x)) - b(\phi)]$ is the Fourier transform of $b(\phi + v(t-r,x)) - b(\phi)$.

Multiplying (5.27) by $e^{2\gamma t}\hat{v}(t,\xi)$ with some constant $\gamma > 0$ to be determined later, integrating the resultant over $[0,t] \times \mathbb{R}^N$, and using the Hölder inequality, we obtain

$$\begin{aligned} & e^{2\gamma t}\|\hat{v}(t)\|^2_{L^2(\mathbb{R}^N)} + 2(D\lambda_1 + \delta - \gamma)\int_0^t e^{2\gamma s}\|\hat{v}(s)\|^2_{L^2(\mathbb{R}^N)} ds \\ & = \|\hat{v}(0)\|^2_{L^2(\mathbb{R}^N)} + 2(1-\lambda_2)\int_0^t e^{2\gamma s}\int_{\mathbb{R}^N} \hat{v}(s,\xi)\mathcal{F}[b(\phi+v) - b(\phi)](s-r,\xi)d\xi ds \\ & \le \|\hat{v}(0)\|^2_{L^2(\mathbb{R}^N)} \\ & \quad + 2(1-\lambda_2)\int_0^t e^{2\gamma s}\|\hat{v}(s)\|_{L^2(\mathbb{R}^N)}\|\mathcal{F}[b(\phi+v) - b(\phi)](s-r)\|_{L^2(\mathbb{R}^N)} ds. \end{aligned} \tag{5.28}$$

Applying the Plancherel equality to (5.28), we have

$$\begin{aligned} & e^{2\gamma t}\|v(t)\|^2_{L^2(\mathbb{R}^N)} + 2(D\lambda_1 + \delta - \gamma)\int_0^t e^{2\gamma s}\|v(s)\|^2_{L^2(\mathbb{R}^N)} ds \\ & \le \|v(0)\|^2_{L^2(\mathbb{R}^N)} \\ & \quad + 2(1-\lambda_2)\int_0^t e^{2\gamma s}\|v(s)\|_{L^2(\mathbb{R}^N)}\|[b(\phi+v) - b(\phi)](s-r)\|_{L^2(\mathbb{R}^N)} ds. \end{aligned} \tag{5.29}$$

When $e < \frac{(1-\lambda_2)p}{D\lambda_1+\delta} < e^2$, the birth rate function $b(u)$ becomes concave upward, which cannot guarantees the global convergence. Here, we have to estimate $b(\phi + v) - b(\phi)$ by the Taylors's expansion as follows, and we may have the local convergence only.

$$|b(\phi+v) - b(\phi)| = \left|b'(\phi)v + \frac{1}{2}b''(\tilde{u})v^2\right| \le |b'(\phi)v| + C|v|^2,$$

where $\tilde{u}$ is a function between ϕ and $\phi + v$, and $|b''(\tilde{u})| \le C$.

Note that,

$$b'(u_+) = \frac{D\lambda_1 + \delta}{1 - \lambda_2}\left(1 - \ln\frac{(1-\lambda_2)p}{D\lambda_1 + \delta}\right) < 0, \tag{5.30}$$

for $e < \frac{(1-\lambda_2)p}{D\lambda_1+\delta} < e^2$, we estimate

$$\begin{aligned}
&\|(b(\phi+v) - b(\phi))(s-r)\|_{L^2(\mathbb{R}^N)} \\
&\le \|b'(\phi)v(s-r)\|_{L^2(\mathbb{R}^N)} + C\|v(s-r)\|^2_{L^2(\mathbb{R}^N)} \\
&= \|b'(\phi)v(s-r)\|_{L^2(\Omega)} + C\|v(s-r)\|^2_{L^2(\Omega)} \\
&= |b'(u_+)|\|v(t-r)\|_{L^2(\Omega)} + C\|v(s-r)\|^2_{L^2(\Omega)} \\
&= \left|1 - \ln\frac{(1-\lambda_2)p}{D\lambda_1+\delta}\right|\|v(t-r)\|_{L^2(\Omega)} + C\|v(s-r)\|^2_{L^2(\Omega)}.
\end{aligned} \tag{5.31}$$

Substituting (5.31) into (5.28), noting $\|v(t)\|_{L^2(\mathbb{R}^N)} = \|v(t)\|_{L^2(\Omega)}$, and applying Cauchy-Schwarz inequality and the change of variable $s - r \to s$, we have

$$\begin{aligned}
&e^{2\gamma t}\|v(t)\|^2_{L^2(\Omega)} + 2(D\lambda_1 + \delta - \gamma)\int_0^t e^{2\gamma s}\|v(s)\|^2_{L^2(\Omega)} ds \\
&\le \|v_0(0)\|^2_{L^2(\Omega)} \\
&\quad + 2\left|1 - \ln\frac{(1-\lambda_2)p}{D\lambda_1+\delta}\right|(D\lambda_1+\delta)\int_0^t e^{2\gamma s}\|v(s)\|_{L^2(\Omega)}\|v(s-r)\|_{L^2(\Omega)} ds \\
&\quad + C\int_0^t e^{2\gamma s}\|v(s)\|_{L^2(\Omega)}\|v^2(t-r)\|_{L^2(\Omega)} \\
&\le \left|1 - \ln\frac{(1-\lambda_2)p}{D\lambda_1+\delta}\right|(D\lambda_1+\delta)\int_0^t e^{2\gamma s}[\|v(s)\|^2_{L^2(\Omega)} + \|v(s-r)\|^2_{L^2(\Omega)}] ds \\
&\quad + CN(T)\int_0^t e^{2\gamma s}[\|v(s)\|^2_{L^2(\Omega)} + \|v(s-r)\|^2_{L^2(\Omega)}] ds + \|v_0(0)\|^2_{L^2(\Omega)} \\
&\le \left|1 - \ln\frac{(1-\lambda_2)p}{D\lambda_1+\delta}\right|(D\lambda_1+\delta)\int_0^t e^{2\gamma s}\|v(s)\|^2_{L^2(\Omega)} ds \\
&\quad + \left|1 - \ln\frac{(1-\lambda_2)p}{D\lambda_1+\delta}\right|(D\lambda_1+\delta)\int_0^t e^{2\gamma(s+r)}\|v(s)\|^2_{L^2(\Omega)} ds
\end{aligned}$$

$$
\begin{aligned}
&+C\int_{-r}^{0} e^{2\gamma(s+r)}\|v_0(s)\|^2_{L^2(\Omega)}ds + \|v_0(0)\|^2_{L^2(\Omega)}\\
&+CN(T)\int_0^t e^{2\gamma s}\|v(s)\|^2_{L^2(\Omega)}ds + CN(T)\int_{-r}^{0} e^{2\gamma(s+r)}\|v_0(s)\|^2_{L^2(\Omega)}ds\\
\le&\left[\left|1-\ln\frac{(1-\lambda_2)p}{D\lambda_1+\delta}\right|(D\lambda_1+\delta)(1+e^{2\gamma r})+CN(T)\right]\int_0^t e^{2\gamma s}\|v(s)\|^2_{L^2(\Omega)}ds\\
&+\|v_0(0)\|^2_{L^2(\Omega)}+\|v_0\|^2_{L^2([-r,0];L^2(\Omega))},
\end{aligned}
\tag{5.32}
$$

where

$$
N(T) := \sup_{(t,x)\in[0,T]\times\Omega} |v(t,x)|.
$$

Organizing (5.32), we have

$$
\begin{aligned}
&e^{2\gamma t}\|v(t)\|^2_{L^2(\Omega)} + [G(\gamma)-CN(T)]\int_0^t e^{2\gamma s}\|v(s)\|^2_{L^2(\Omega)}ds\\
&\le C\left(\|v_0(0)\|^2_{L^2(\Omega)}+\|v_0\|^2_{L^2([-r,0];L^2(\Omega))}\right),
\end{aligned}
\tag{5.33}
$$

where

$$
G(\gamma) := (D\lambda_1+\delta)\left[1-\left|1-\ln\frac{(1-\lambda_2)p}{D\lambda_1+\delta}\right|\right] \tag{5.34}
$$

$$
-2\gamma - 2(D\lambda_1+\delta)\left|1-\ln\frac{(1-\lambda_2)p}{D\lambda_1+\delta}\right|\left(e^{2\gamma r}-1\right). \tag{5.35}
$$

Note that $e<\frac{(1-\lambda_2)p}{D\lambda_1+\delta}<e^2$, then one can easily see that $0<\left|1-\ln\frac{(1-\lambda_2)p}{D\lambda_1+\delta}\right|<1$, which in turn implies

$$
(D\lambda_1+\delta)\left[1-\left|1-\ln\frac{(1-\lambda_2)p}{D\lambda_1+\delta}\right|\right]>0,\quad 2(D\lambda_1+\delta)\left|1-\ln\frac{(1-\lambda_2)p}{D\lambda_1+\delta}\right|>0. \tag{5.36}
$$

Thus, we can take $0<\gamma\ll 1$ sufficiently small, such that

$$
G(\gamma)>0.
$$

Furthermore, let $N(T)\ll 1$ be sufficiently small, we can guarantee

$$
G(\gamma)-CN(T)>0.
$$

This combining (5.33) gives

$$\|v(t)\|^2_{L^2(\Omega)} \le Ce^{-2\gamma t}\Big(\|v_0(0)\|^2_{L^2(\Omega)} + \|v_0\|^2_{L^2([-r,0];L^2(\Omega))}\Big). \tag{5.37}$$

By the standard continuation argument, we know that the ansatz $N(T) \ll 1$ can be guaranteed by assuming that the initial data

$$\|(u_0-\phi)(0)\|_{L^2(\Omega)} + \|u_0-\phi\|_{L^2([-r,0];L^2(\Omega))}$$

is small enough. The proof is complete. □

6. Numerical simulations

In this section, we conduct numerical simulations to support the theoretical results obtained above. Here, we will start by presenting the algorithmic section.

6.1. Algorithms

We would like to consider the 1-dimensional case in the following experiments. In this case, $N = 1$ will be utilized in (1.1). In the computational process, we primarily utilize numerical integration and numerical differentiation techniques. Let $\{x_j\}_{j=1}^m$ and $\{y_k\}_{k=1}^m$ be sets of points obtained from the equidistant partition of the interval $[-M, M] = [-10, 10]$ (position subintervals have equal lengths of $\Delta x = \Delta y = 0.01$) and $\{t_i\}_{i=1}^n$ ($t_0 = 0$) represent a collection of the equidistant partition points within finite time $[0, T]$, $T > 0$ (time subintervals have equal lengths of $\Delta t = 0.01$). The initialization is as follows,

$$u_0(x,t) = \begin{cases} (x-5)(x+5) + (t-r)(t+r), & \text{if } -5 < x \le 5 \text{ and } -r < t \le r, \\ 0, & \text{otherwise.} \end{cases} \tag{6.1}$$

The forms of the kernels J_1 and J_2 in the two convolution terms of (1.1) are as follows,

$$J_1(y) = \frac{1}{1+y^2}, \quad J_2(y) = e^{-y^2}, \quad y \in \mathbb{R}. \tag{6.2}$$

We begin by discretizing the temporal dimension, opting for a forward-difference method due to the absence of spatial derivatives in the equation. i.e., at a moment $t > 0$,

$$\frac{\partial u(t,x)}{\partial t} \approx \frac{u(t+\Delta t, x) - u(t,x)}{\Delta t}. \tag{6.3}$$

Since the data is obtained within a finite interval $[-M, M]$, the discretization of the two integrals in the model is as follows,

$$\int_{-M}^{M} J_1(x-y)[u(t,y)-u(t,x)]dy \approx \sum_{k=1}^{m} J_1(x-y_k)[u(t,y_k)-u(t,x)] \cdot \Delta y, \tag{6.4}$$

and

$$\int_{-M}^{M} J_2(x-y)f(u(t-r,y))dy \approx \sum_{k=1}^{m} J_2(x-y_k)f(u(t-r,y_k)) \cdot \Delta y. \tag{6.5}$$

Let $u(t,x) = u_0(t,x)$, $t \in [-r,0]$. According to (6.4)–(6.5), we obtain the following approximate iterative process, for $i = 0, 1, \ldots, n$, $j = 1, \ldots, m$,

$$u(t_{i+1}, x_j) = u(t_i, x_j) + \Delta t \cdot (D \cdot I_1(t_i, x_j) + I_2(t_i, x_j) - \delta u(t_i, x_j)), \tag{6.6}$$

where

$$I_1(t_i, x_j) = \sum_{k=1}^{m} J_1(x_j - y_k)[u(t_i, y_k) - u(t_i, x_j)] \cdot \Delta y,$$

$$I_2(t_i, x_j) = \sum_{k=1}^{m} J_2(x_j - y_k)f(u(t_i - r, y_k)) \cdot \Delta y,$$

and $r > 0$ denotes the time-delay. So far, we have provided the iterative format for numerically solving the forward problem. The following subsection is devoted to the analysis of numerical results. All notations in our experiments remind the same as the contexts, i.e., we denote a as the coefficient in the birth function (1.4), D as the diffusion rate, and p, δ as the birth/death rates.

6.2. Numerical results

We employ various birth rates p and death rates δ, ensuring the solutions to the diffusion equations eventually reach different convergence states. In terms of background significance, if the solution converges to a zero steady state, it signifies the eventual extinction of the biological population. On the other hand, convergence to a non-trivial steady state indicates that the population density tends to stabilize. In the following figures, $a = \log(2)$ denotes the parameter in the birth function $b(u) = pue^{-au}$, while $D = 1$ represents the diffusion coefficient of the biological population. Additionally, it is worth explaining that, in the crucial term $p(1-\lambda_2)(D\lambda_1+\delta)^{-1}$, determining the specific values of the eigenvalues λ_1 and λ_2 in numerical simulations poses considerable challenges. This is due to the fact that they are associated with a variational minimization problem related to the spatial region of position x and kernel functions J_1 and J_2. Nevertheless, we are aware that these eigenvalues remain less than 1.

We first consider the smaller time delay $r = 3$. Fig. 1 is the three-dimensional representations of the solution u with respect to time t and position x with $0 < p(1-\lambda_2)(D\lambda_1+\delta)^{-1} < 1$ and $1 < p(1-\lambda_2)(D\lambda_1+\delta)^{-1} \le e^2$, respectively. The terminal moments are $T = 10$ and $T = 30$, respectively. When $t \in [-r, 0)$, it represents that the biological individuals are still in an immature state, i.e., the time delay. By comparing the two sets of experiments, despite the same initial value is applied, the left graph of Fig. 1 ultimately converges to the zero steady state under the condition of $0 < p(1-\lambda_2)(D\lambda_1+\delta)^{-1} < 1$, where $p = 1$ and $\delta = 5$. However, as the birth rate $p = 1.5$ and death rate $\delta = 0.5$ satisfying $1 < p(1-\lambda_2)(D\lambda_1+\delta)^{-1} < e^2$ in the right graph of Fig. 1, the system ultimately reaches a non-trivial steady state. According to these results, it is evident that the ultimate equilibrium of the biological population is minimally affected by the

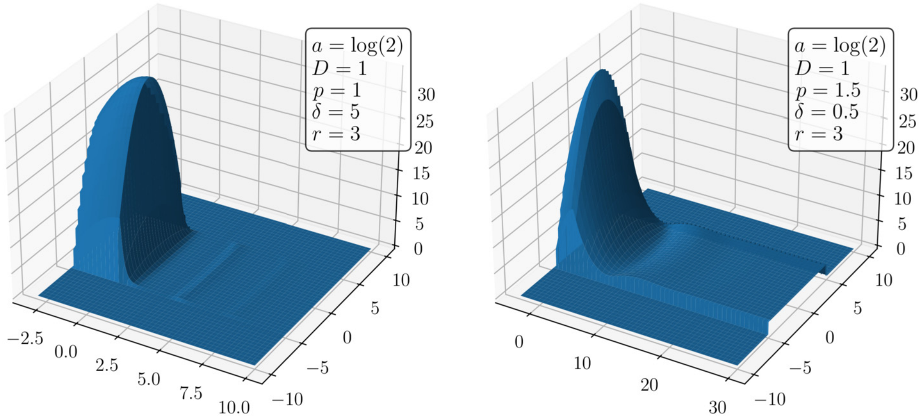

Fig. 1. Two types of convergence in 3D: the left is the convergence to the zero steady state, once $0 < p(1-\lambda_2)(D\lambda_1 + \delta)^{-1} < 1$; and the right is the convergence to the non-trivial steady state, once $1 < p(1-\lambda_2)(D\lambda_1+\delta)^{-1} \le e^2$.

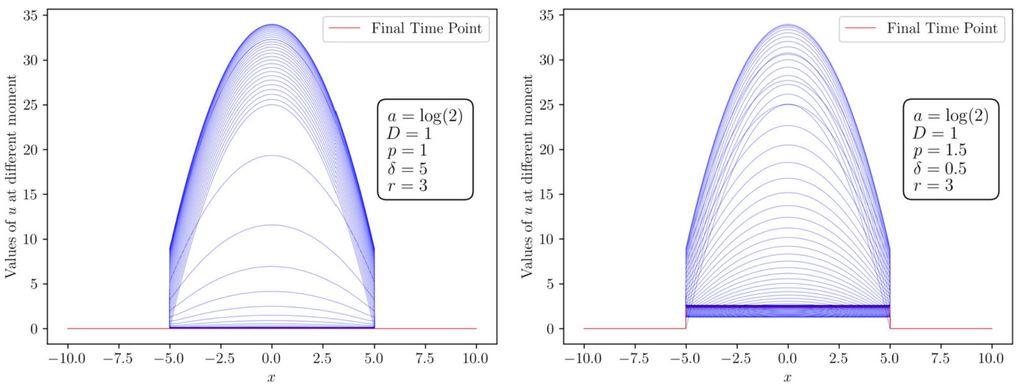

Fig. 2. Two types of convergence in 2D: the left is the convergence to the zero steady state, once $0 < p(1-\lambda_2)(D\lambda_1 + \delta)^{-1} < 1$; and the right is the convergence to the non-trivial steady state, once $1 < p(1-\lambda_2)(D\lambda_1+\delta)^{-1} < e^2$. (For interpretation of the colors in the figure(s), the reader is referred to the web version of this article.)

initial conditions $u_0(t,x)$. The crucial determinants lie in the parameters p and δ, corresponding to the birth and death rates. If p and δ are in relative equilibrium, the population would maintain a positive constant. When δ is significantly larger than p, it results in the population density tending towards zero, corresponding to the fact of biological extinction.

In Fig. 2, we extract several time points to study the steady states to which solutions eventually converge under different birth and death rates. Each of sub-figures in Fig. 2 displays the convergence tendency by blue lines. We illustrate the relationship between u and x at different time points. Both solutions reach different converged states after certain periods, with the red line representing the final steady state in Figs. 2. The left graph of Figs. 2 represents the case where the solution converges to the trivial steady state under the condition $0 < p(1-\lambda_2)(D\lambda_1+\delta)^{-1} < 1$, where $p = 1$ and $\delta = 4.5$. In this scenario, it implies that the population eventually leads to extinction. The right graph of Figs. 2 illustrates the case where the solution to the equation converges to a non-trivial steady state when $p = 1$, $\delta = 0.1$ and $1 < p(1-\lambda_2)(D\lambda_1+\delta)^{-1} < e^2$, signifying that the population density stabilizes at a non-zero state. In order to demonstrate the convergence process more explicitly, the states in several moments are provided in Fig. 3.

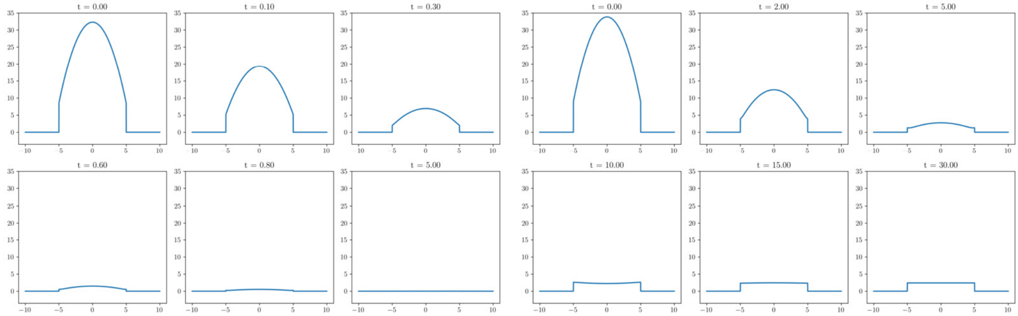

Fig. 3. Different converging tendencies under different thresholds: the left is the solution u converging to the zero steady state, once $0 < p(1-\lambda_2)(D\lambda_1+\delta)^{-1} < 1$; the right is the solution u converging to a non-trivial steady state, once $1 < p(1-\lambda_2)(D\lambda_1+\delta)^{-1} < e^2$.

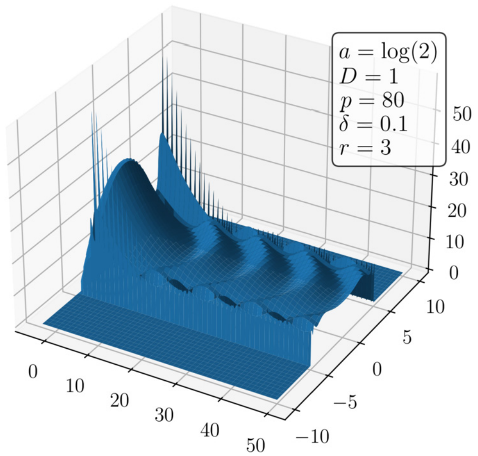

Fig. 4. A larger birth rate causes the solution to oscillate, when $p(1-\lambda_2)(D\lambda_1+\delta)^{-1} \geq e^2$ with a small time-delay $r = 3$.

Considering the case of further increasing $p(1-\lambda_2)(D\lambda_1+\delta)^{-1}$, the convergence of the solution is no longer guaranteed. We have experimented with larger birth rates and smaller death rates in Figs. 4 and Fig. 5. As can be seen in the figures, the solution oscillates when $p = 80$, $\delta = 0.1$ such that $p(1-\lambda_2)(D\lambda_1+\delta)^{-1} > e^2$. Fig. 4 gives the numerical solution of the equation under $t \in [-3, 50]$, while Fig. 5 enables a more intuitive view of the oscillations. The practical implication is that the large birth rate leads to population densities falling out of the steady state.

Even after increasing the time delay, the solution u does not converge under the same initial value. The experiment in Fig. 6 builds on Fig. 7 by increasing the time delay to $r = 16$. As can be observed, the amplitude of the solution is more drastic.

7. Discussion

In this section, we are going to use the above theoretical and numerical results to interpret the population dynamics represented by the nonlocal reaction-diffusion equation (1.1). The birth rate p and the death rate δ play the crucial roles for the population dynamics. When the death

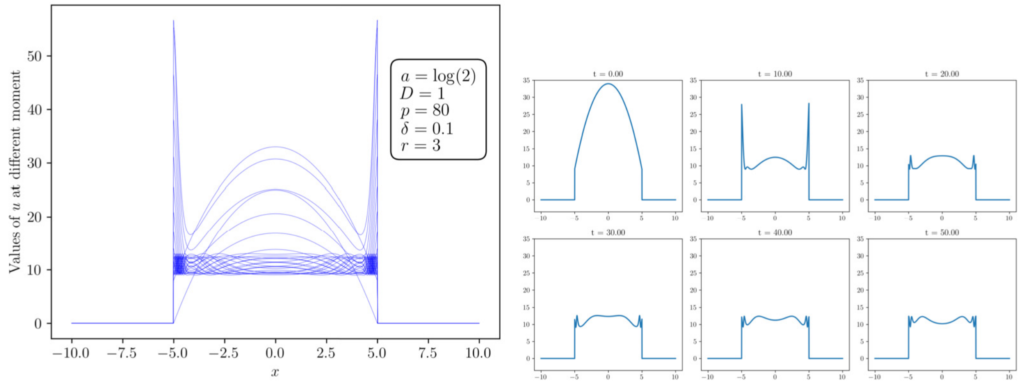

Fig. 5. Oscillation of the solution $u(t,x)$ in different time, when $p(1-\lambda_2)(D\lambda_1+\delta)^{-1} \geq e^2$ with a small time-delay $r = 3$: the left is the relationships between u and x at several moments; the right is the detailed evolution of u when the birth rate is significantly larger than the death rate.

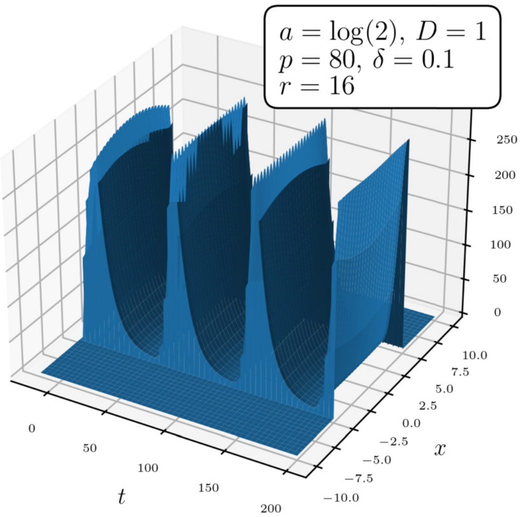

Fig. 6. The solution u under the larger birth and the small death rate in 3D, when $p(1-\lambda_2)(D\lambda_1+\delta)^{-1} \geq e^2$ with a large time-delay $r = 16$.

rate δ is bigger than the birth rate p such that $0 < p(1-\lambda_2)(D\lambda_1+\delta)^{-1} < 1$, then, no matter how large the initial data $u_0(x)$ are, no matter what size the mature age (delay time) r is for the single species, the solution $u(t,x)$ will time-exponentially converge to zero for any initial data, namely, the population of the single species will gradually perish, where the domain Ω for single species to live and the probabilities J_1 and J_2 of single species moving-in and moving-out make some minor affection, because the principal eigenvalues $\lambda_i = \lambda_i(\Omega, J_i)$ for $i = 1, 2$ depend on Ω and $J_i(x)$. On the other hand, when the birth rate p is a bit larger than the death rate δ such that $1 < p(1-\lambda_2)(D\lambda_1+\delta)^{-1} \leq e$, the solution $u(t,x)$ will globally converge to the non-trivial steady-state $\phi(x)$ in (3.3), namely, the population of single species will gradually tend to the non-trivial steady-state, where the population becomes a constant $u_+ = \frac{1}{a}\ln\frac{(1-\lambda_2)p}{D\lambda_1+\delta} > 0$ in the interior domain of Ω, and it is zero on the boundary $\partial\Omega$ because the zero boundary condition

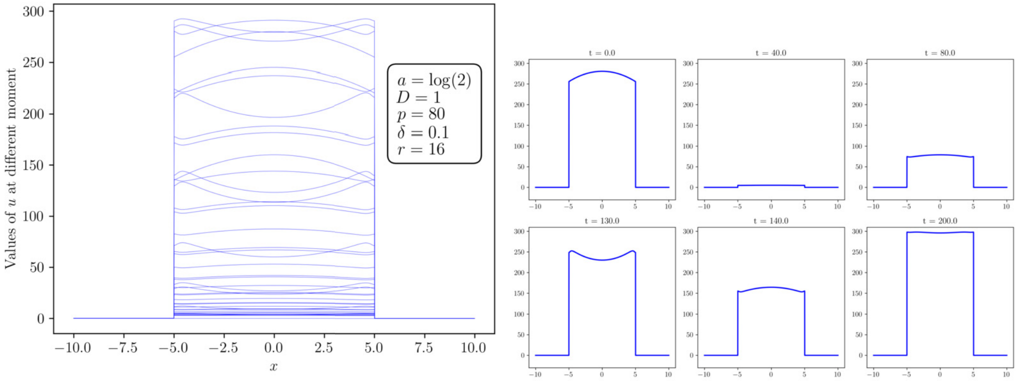

Fig. 7. Oscillatory solutions with a large time delay $r = 16$ in 2D, once $p(1-\lambda_2)(D\lambda_1+\delta)^{-1} \geq e^2$: the left is the solution u to the zero steady state; the right is the solution u to a non-trivial steady state.

means there is a close fence on the boundary to stop the single species to move out. When $e < p(1-\lambda_2)(D\lambda_1+\delta)^{-1} < e^2$, we theoretically proved that, once the initial population is not a big change around u_+, then the population $u(t,x)$ will still behave like the steady-state u_+ in the interior domain Ω after a long time. However, our numerical results indicate that, even the distribution of the initial population around u_+ is chaotic and big, the population of the single species will finally tend to the steady-state u_+ in the inside domain Ω. Moreover, once $p(1-\lambda_2)(D\lambda_1+\delta)^{-1} > e^2$, the numerical results demonstrate that the distribution of population will be chaotic and oscillatory in the domain Ω all the time, and the oscillations for the population distribution will be large if the delay-time (mature age) r is big, no matter how stable the initial distribution of population is.

Acknowledgments

The paper was done when L. Yang studied at McGill University as a PhD Trainee supported by China Scholarship Council (CSC) (No. 202106480020), and H. Hu visited McGill University as a visiting scholar supported by China Scholarship Council (CSC) (No. 202007535001). Both of them would like to express their sincere thanks for the hospitality of McGill University and CSC. The research of H. Hu was supported in part by NSFC of China No. 11801039, 12271087, and the Science and Technology Department of Jilin Province of China (No. YDZJ202501ZYTS598). The research of M. Mei was supported in part by NSERC Grant of Canada RGPIN-2022-03374 and NSFC of China No. W2431005. The research of D. Xu was supported in part by the NSFC of China No. 11871435, 12371428, and Fundamental Research Funds for the Chinese Central Universities, SUFE.

Data availability

No data was used for the research described in the article.

References

[1] G. Albert, G. Bellettini, A non-local anisotropic model for phase transitions: asymptotic behavior of rescaled energies, Eur. J. Appl. Math. 9 (1988) 261–284.

[2] F. Andreu-Vaillo, Nonlocal Diffusion Problems, vol. 165, American Mathematical Soc., 2010.
[3] P.W. Bates, P.C. Fife, X. Ren, X. Wang, Traveling waves in a convolution model for phase transitions, Arch. Ration. Mech. Anal. 138 (1997) 105–136.
[4] P.W. Bates, G. Zhao, Existence, uniqueness and stability of the stationary solution to a nonlocal evolution equation arising in population dispersal, J. Math. Anal. Appl. 332 (2007) 428–440.
[5] G.A.-G. Bellettini, A nonlocal anisotropic model for phase transition, Math. Ann. 310 (1998) 527–560.
[6] H. Berestycki, J. Coville, H.-H. Vo, Persistence criteria for populations with non-local dispersion, J. Math. Biol. 72 (2006) 1693–1745.
[7] I.H. Biswas, E.R. Jakobsen, K.H. Karlsen, Error estimates for finite difference-quadrature schemes for a class of nonlocal Bellman equations with variable diffusion, Contemp. Math. 429 (2007) 19.
[8] M. Bodner, J.J. Velázquez, An integro-differential equation arising as a limit of individual cell-based models, J. Differ. Equ. 222 (2006) 341–380.
[9] C. Carrillo, P. Fife, Spatial effects in discrete generation population models, J. Math. Biol. 50 (2005) 161–188.
[10] E. Chasseigne, M. Chaves, J.D. Rossi, Asymptotic behavior for nonlocal diffusion equations, J. Math. Pures Appl. 86 (2006) 271–291.
[11] I-L. Chern, M. Mei, X. Yang, Q. Zhang, Stability of non-monotone critical traveling waves for reaction-diffusion equations with time-delay, J. Differ. Equ. 259 (2015) 1503–1541.
[12] J. Coville, On a simple criterion for the existence of a principal eigenfunction of some nonlocal operators, J. Differ. Equ. 249 (2010) 2921–2953.
[13] J. Coville, Harnack type inequality for positive solution of some integral equation, Ann. Mat. Pura Appl. 191 (2012) 503–528.
[14] J. Coville, Singular measure as principal eigenfunction of some nonlocal operators, Appl. Math. Lett. 26 (2013) 831–835.
[15] J. Coville, Nonlocal refuge model with a partial control, Discrete Contin. Dyn. Syst. 35 (2015) 1421–1446.
[16] J. Coville, J. Dávila, S. Martínez, Pulsating fronts for nonlocal dispersion and KPP nonlinearity, Ann. Inst. Henri Poincaré C, Anal. Non Linéaire 30 (2013) 179–223.
[17] Q. Du, M. Gunzburger, R. Lehoucq, K. Zhou, Analysis and approximation of nonlocal diffusion problems with volume constraints, SIAM Rev. 54 (2012) 667–696.
[18] N. Fournier, P. Laurençot, Well-posedness of Smoluchowski's coagulation equation for a class of homogeneous kernels, J. Funct. Anal. 233 (2006) 351–379.
[19] J. García-Melián, F. Quirós, Fujita exponents for evolution problems with nonlocal diffusion, J. Evol. Equ. 10 (2010) 147.
[20] G. Gilboa, S. Osher, Nonlocal linear image regularization and supervised segmentation, Multiscale Model. Simul. 6 (2007) 595–630.
[21] R. Huang, M. Mei, Y. Wang, Planar traveling waves for nonlocal dispersion equation with monostable nonlinearity, Discrete Contin. Dyn. Syst. 32 (2012) 3621–3649.
[22] R. Huang, M. Mei, Z. Wang, Threshold convergence results for a nonlocal time-delayed diffusion equation, J. Differ. Equ. 364 (2023) 76–106.
[23] R. Huang, M. Mei, K. Zhang, Q. Zhang, Asymptotic stability of non-monotone traveling waves for time-delayed nonlocal dispersion equations, Discrete Contin. Dyn. Syst. 36 (2016) 1331–1353.
[24] L.I. Ignat, T.I. Ignat, Long-time behavior for a nonlocal convection diffusion equation, J. Math. Anal. Appl. 455 (2017) 816–831.
[25] L.I. Ignat, J.D. Rossi, A. San Antolin, Lower and upper bounds for the first eigenvalue of nonlocal diffusion problems in the whole space, J. Differ. Equ. 252 (2012) 6429–6447.
[26] E.R. Jakobsen, K.H. Karlsen, Continuous dependence estimates for viscosity solutions of integro-PDEs, J. Differ. Equ. 212 (2005) 278–318.
[27] Y. Jiang, B. Rubino, K. Zhang, Asymptotic behavior of solutions for time-delayed nonlocal dispersion equations with Dirichlet boundary, Appl. Anal. 101 (2022) 5684–5699.
[28] S. Kindermann, S. Osher, P.W. Jones, Deblurring and denoising of images by nonlocal functionals, Multiscale Model. Simul. 4 (2005) 1091–1115.
[29] C.-K. Lin, C.-T. Lin, Y. Lin, M. Mei, Exponential stability of non-monotone traveling waves for Nicholson's blowflies equation, SIAM J. Math. Anal. 46 (2014) 1053–1084.
[30] A. Mogilner, L. Edelstein-Keshet, A non-local model for a swarm, J. Math. Biol. 38 (1999) 534–570.
[31] S. Pan, W.-T. Li, G. Lin, Existence and stability of traveling wavefronts in a nonlocal diffusion equation with delay, Nonlinear Anal., Theory Methods Appl. 72 (2010) 3150–3158.
[32] A. Solar, Stability of non-monotone and backward waves for delay non-local reaction-diffusion equations, Discrete Contin. Dyn. Syst. 39 (2019) 5799–5823.

[33] J.W.-H. So, J. Wu, X. Zou, A reaction–diffusion model for a single species with age structure. I Travelling wavefronts on unbounded domains, Proc. R. Soc. Lond. Ser. A 457 (2001) 1841–1853.
[34] J.W.-H. So, Y. Yang, Dirichlet problem for the diffusive Nicholson's blowflies equation, J. Differ. Equ. 150 (1998) 317–348.
[35] E.M. Stein, G. Weiss, Introduction to Fourier Analysis on Euclidean Spaces, Princeton University Press, 1971.
[36] T. Xu, S. Ji, R. Huang, M. Mei, J. Yin, Theoretical and numerical studies on global stability of traveling waves with oscillations for time-delayed nonlocal dispersion equations, Int. J. Numer. Anal. Model. 17 (2020) 68–86.
[37] H. Yagisita, Existence and nonexistence of traveling waves for a nonlocal monostable equation, Publ. Res. Inst. Math. Sci. 45 (2010) 925–953.
[38] G.-B. Zhang, Non-monotone traveling waves and entire solutions for a delayed nonlocal dispersal equation, Appl. Anal. 96 (2017) 1830–1866.
[39] G.-B. Zhang, Global stability of non-monotone traveling wave solutions for a nonlocal dispersal equation with time delay, J. Math. Anal. Appl. 475 (2019) 605–627.